Published in : Polymer Chemistry (2019), vol. 10, n°23, pp. 3055–3065
DOI: 10.1039/c9py00020h
Status : Postprint (Author's version)

PRECISION DESIGN OF VINYL AMINE AND VINYL ALCOHOL-BASED COPOLYMERS VIA COBALT-MEDIATED RADICAL POLYMERIZATION

Pierre Stiernet[a], Christine Jérôme[a] and Antoine Debuigne[a]

[a]*Center for Education and Research on Macromolecules (CERM), CESAM-Research Unit, University of Liège (ULiege), Sart-Tilman, Allée de la Chimie 3, Bat. B6a, B-4000 Liège, Belgium.*

Abstract

Poly(vinyl alcohol) (PVA) and poly(vinyl amine) (PVAm) are major industrial polymers involved in countless applications taking advantage of their ability to establish hydrogen bonds and, for the latter, to create charges along the polymer's backbone upon protonation. Although combining vinyl alcohol and vinyl amine units in specific proportions within copolymers should allow precise tuning of their properties and enlarge the scope of their use, the controlled synthesis of poly(VAm-*co*-VA)s has been completely disregarded so far. In this context, we report a straightforward strategy for preparing the aforementioned copolymers via cobalt-mediated radical copolymerization of vinyl acetate (VAc) and vinyl acetamide (NVA) followed by hydrolysis. Copolymerization conditions were optimized to produce poly(NVA-*co*-VAc) with predictable molar mass, low dispersity and precise composition. Reactivity ratios were also determined to gain insight into the distribution of the amine and alcohol moieties along the backbone. Depending on the hydrolysis treatment applied to poly(NVA-*co*-VAc), unprecedented well-defined poly(VAm-*co*-VA)s and poly(NVA-*co*-VA)s were achieved via full deprotection of the precursor and selective hydrolysis of its esters, respectively.

Introduction

Polymers containing large numbers of alcohol and/or amine functions are valuable for several applications, notably due to their hydrogen bond capacity and the protonation ability of the amino groups. Among vinyl polymers, poly(vinyl alcohol) (PVA) and poly(vinyl amine) (PVAm) present, respectively, the highest density of pendant alcohol and amine moieties. In particular, PVA is a major industrial polymer whose production exceeds one million metric tons per year. This water soluble macromolecule covers a vast range of uses, notably in the biomedical area.[1–3] PVAms are another important class of polymers that is valued in surface and interface modification,[4] gas separation,[5,6] flocculation,[7] carbon dioxide capture,[8] water purification,[9–11] paper strengthening[12] or gene transfection.[13,14] These applications benefit from specific properties of PVAm like affinity for many supports, high hydrogen bond capacity, and ability to complex metals and polyelectrolytes. PVAm can also undergo several chemical modifications such as alkylation, ring opening of epoxides or Michael

Published in : Polymer Chemistry (2019), vol. 10, n°23, pp. 3055–3065
DOI: 10.1039/c9py00020h
Status : Postprint (Author's version)

addition, which allows adjusting its properties and fulfilling the requirements of specific applications.[15–21]

In terms of synthesis, PVA and PVAm share similarities (**Scheme 1**). The instability of vinyl alcohol and vinyl amine, which are involved in a tautomeric equilibrium with the corresponding ketone[22] and imine,[23] prohibits their direct polymerization and requires masking of the alcohol and the amine functions with protective groups during the polymerization process. Typically, the industrial production of PVA consists of the free radical polymerization (FRP) of vinyl acetate (VAc) followed by methanolysis of the pendant esters.[1,2] Likewise, FRP of acyclic *N*-vinyl amides, namely *N*-vinyl formamide (*N*VF)[24–26] or *N*-vinyl acetamide (*N*VA),[27–29] followed by hydrolysis of the pendant amides gives access to PVAm. Alternatively, PVAm can be prepared by hydrazinolysis of poly (*N*-vinyl phthalimide) (P*N*VPi), but the atom economy of this approach is low.[30] Although reports on the preparation of statistical poly(VAm-*co*-VA) *via* subsequent FRP of *N*VF/VAc and hydrolysis are scarce,[31] some poly(VAm-*co*-VA)s have been prepared accordingly and commercialized, notably as cold-water-soluble PVA-based materials.[32] Crosslinking of the latter notably produced P(VA-VAm) hydrogels with improved stability.[32] However, these syntheses suffer from poor control of the molecular parameters, composition and distribution of the amine and alcohol functions along the copolymer chains.

Nowadays, the synthesis of well-defined PVA and PVAm can be achieved through reversible deactivation radical polymerization (RDRP) of vinyl esters[33–35] and acyclic vinyl amides[36,37] or vinyl phtalimides.[38] These monomers belong to the socalled "less activated monomers" (LAMs) category and represent a challenge for RDRP because they are deprived of a radical stabilizing group on their double bonds making more difficult the reactivation of the dormant species and the release of the active radicals. However, some RDRP methods offer decent to excellent control of their radical polymerization. For example, the reversible addition fragmentation chain transfer (RAFT) based on xanthates produces well-defined PVAc[35] and P*N*VPI[38] leading to PVA[35] and PVAm[38] with controlled molecular parameters. However, although the RAFT of cyclic *N*-vinyl amides like *N*-vinylpyrrolidone (*N*VP) and *N*-vinylcaprolactam (*N*VCL) is reported,[39] to our knowledge, the controlled polymerization of acyclic *N*-vinyl amides like *N*VF or *N*-vinyl acetamide (*N*VA) has never been described by this method. In contrast, cobalt-mediated radical polymerization (CMRP)[40–42] shows excellent control of the polymerization of both vinyl esters[43–45] and acyclic *N*-vinyl amides including *N*VA[36,37] and *N*-methyl vinyl acetamide (*N*MVA).[14,36,46] In this case, bis(acetylacetonato)cobalt(II) ($Co(acac)_2$) was used as a moderating species which reversibly traps the growing radical chains. Recently, some of these PVAms with controlled molecular parameters have been used as gene transfection agents and have demonstrated a high DNA transfection level in combination with high cell viability.[14,47]

In this work, considering the great importance of both PVA and PVAm on the polymer market and the opportunity to enlarge the scope of their applications by combining vinyl amine and vinyl alcohol units in a single polymer chain, we explored for the first time the synthesis of statistical poly(VAm-*co*-VA)s with controlled molar mass and composition. In particular, we developed a two-step process based on the cobalt-mediated radical copolymerization of *N*VA and VAc followed by hydrolysis. The effect of the comonomer feed on the level of control is notably discussed. Moreover, the reactivity ratios were determined in order to gain insight into the distribution of the comonomers along the chain. Finally, acidic and basic hydrolysis procedures of the poly(*N*VA-*co*-VAc)s were optimized paving the way to unprecedented tailor-made poly(VAm-*co*-VA) and poly(*N*VA-*co*-VA) copolymers, respectively.

Published in : Polymer Chemistry (2019), vol. 10, n°23, pp. 3055–3065
DOI: 10.1039/c9py00020h
Status : Postprint (Author's version)

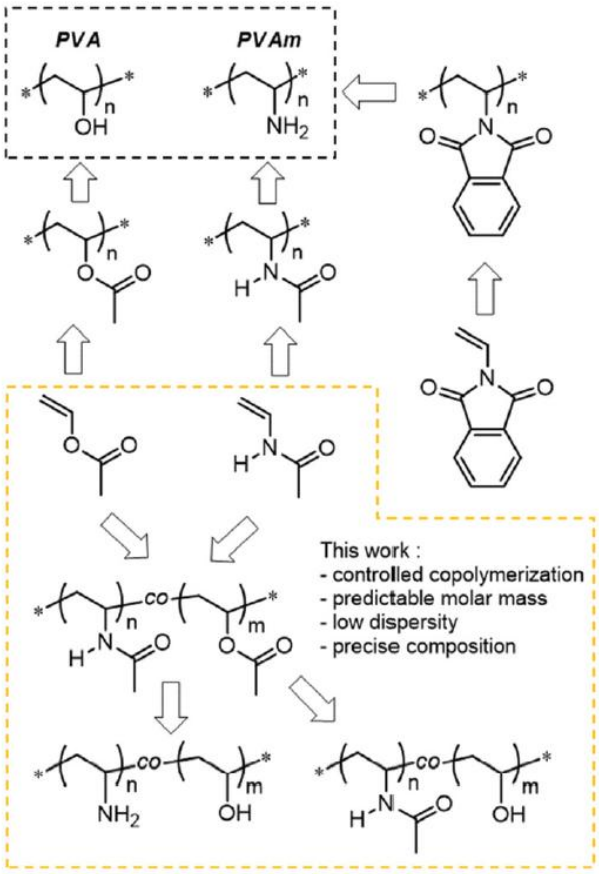

Scheme 1. General strategies for the synthesis of poly(vinyl alcohol), poly(vinyl amine) and the corresponding copolymers.

Experimental section

MATERIALS

N-Vinyl acetamide (*N*VA) (>98%, TCI), cobalt(II) acetylacetonate ($Co(acac)_2$) (97%, Acros), 2,2,6,6-tetramethylpiperidine 1-oxyl (TEMPO) (98%, Aldrich), and 2,2'-azobis(4-methoxy-2,4dimethyl valeronitrile) (V-70, $t_{\frac{1}{2}}$ = 10 h at 30 °C) (>98%, Wako) were used as received. Vinyl acetate (VAc) (>99%, Aldrich) was dried under calcium hydride, purified by distillation under reduced pressure and degassed by a freeze-drying cycle under vacuum. Propanethiol (PrSH) (99%, Aldrich) and dichloromethane (CH_2Cl_2) (p.a.) were degassed by bubbling argon for 30 min. Dimethylformamide (DMF) was dried on molecular sieves and degassed by bubbling argon for 30 minutes. The alkyl–cobalt(III) adduct initiator ($PVAc_{<4}$-$Co(acac)_2$, [$Co(acac)_2$-$(CH(OAc)-CH_2)_{<4}R_0$], R_0 being the primary radical generated by 2,2'-azo-bis(4-methoxy-2,4-dimethyl valeronitrile) (V-70, Wako), was prepared as described previously[44] and stored as a CH_2Cl_2 solution at −20 °C under argon. Dialysis was carried out with a Spectra/Por dialysis membrane (Pre-treated RC Tubing 1 kDa, 3.5 kDa and 8 kDa). The acid digestion vessel (23 mL) used for hydrolysis reactions was purchased from Parr.

Published in : Polymer Chemistry (2019), vol. 10, n°23, pp. 3055–3065
DOI: 10.1039/c9py00020h
Status : Postprint (Author's version)

CHARACTERIZATION

Polymers were analyzed by size exclusion chromatography (SEC) in dimethylformamide (DMF) containing LiBr (0.025 M) at 55 °C (flow rate: 1 mL min^{-1}) with a Waters chromatograph equipped with three columns (Waters Styragel PSS GRAM 1000 Å (×2), 30 Å), a dual λ absorbance detector (Waters 2487) and a refractive index detector (Waters 2414). A polystyrene calibration was used. ^{1}H NMR spectra were recorded at 298 K with a Bruker spectrometer (400 MHz) and treated with MestreNova software. IR spectra were recorded on Thermo Fisher Scientific Nicolet IS5 equipped with an ATR ID5 module using a diamond crystal (650 cm^{-1}–4000 cm^{-1}). Residual cobalt content in the copolymers were measured by inductively coupled plasma (ICP) with Varian 720-E5 apparatus.

CMRP OF NVA AND VAC

A solution of alkyl–cobalt(III) initiator ($PVAc_{<4}$-$Co(acac)_2$) in CH_2Cl_2 (1.0 mL of a 0.088 M stock solution, 0.088 mmol) was taken in a flask under argon and evaporated to dryness under reduced pressure at room temperature followed by the addition of a degassed solution of NVA (1.9 g, 22 mmol) and VAc (2 mL, 1.9 g, 22 mmol) in dry DMF (3.9 mL). The reaction flask was then heated at 40 °C. As a reference, a sample was withdrawn at the initial stage of the reaction and analyzed by ^{1}H NMR in MeOD. Then, samples were regularly picked out of the flask and added with traces of TEMPO. The monomer conversion and the molecular parameters of the polymer were characterized by ^{1}H NMR in MeOD and SEC in DMF, respectively. After 8 h, the overall conversion reached 47% and the polymerization was quenched by the addition of 100-fold of TEMPO compared to cobalt. The final copolymer was purified by precipitation in acetone followed by dialysis in methanol (membrane 3.5 kDa). The copolymer was then dried under vacuum and characterized by ^{1}H NMR in MeOD and SEC in DMF ($M_{n,SEC\ DMF\ cal\ PS}$ = 32 900 g mol^{-1}, $Đ_{SEC\ DMF\ cal\ PS}$ = 1.65).

Similar experiments were carried out with different initial comonomer compositions (f°_{NVA} = 0:3; 0:5 and 0:7), but also at different concentrations (1 g of NVA per mL of DMF instead of 1 g of comonomers per mL of DMF).

DETERMINATION OF THE REACTIVITY RATIOS

In order to determine the reactivity ratios of the CMRP of NVA/VAc, five copolymerization experiments involving different comonomer ratios (0:1 < f°_{NVA} < 0:9) were initiated with the alkyl cobalt initiator at 40 °C in DMF as described above. As a reference, a sample was withdrawn at the initial stage of the reaction and analyzed by ^{1}H NMR in MeOD. Copolymerizations were stopped at a low conversion by the addition of TEMPO in order to avoid significant composition drift. Conversions were determined by ^{1}H NMR in MeOD. The copolymers were purified by precipitation in acetone (when f°_{NVA} > 0:5) or in diethylether (when f°_{NVA} < 0:5) followed by dialysis in MeOH using a 1 kDa membrane and drying at 50 °C under reduced pressure. The molar fraction of NVA and VAc in the copolymer was determined by ^{1}H NMR in MeOD. These data, provided in **Table S1†**, were then used for the determination of the reactivity ratios *via* three methods.

Published in : Polymer Chemistry (2019), vol. 10, n°23, pp. 3055–3065
DOI: 10.1039/c9py00020h
Status : Postprint (Author's version)

We used the Fineman–Ross linearization method[48] which generates a straight line whose slope and intercept with the ordinate (Y-axis) correspond, respectively, to r_1 and r_2 (eqn (1)). The Kelen–Tüdos method[49] was also considered, which involves parameters η and ζ, and mathematical functions of the mole ratios in the monomer feed (f) and in the copolymer (F) and of a parameter α calculated on the basis of the lowest and highest values of (f^2/F). The determination of r_1 and r_2 is made possible by the extrapolation and the interception at $\xi = 1$ and $\xi = 0$, giving, respectively, r_1 and ($1r_2/\alpha$) (eqn (2)). The last method is the non-linear least squares method[50,51] using the Mayo–Lewis equation (eqn (3)).

$$f\,(F - 1)/F = r_1(f^2/F) - r_2, \qquad (1)$$

where $f = f_1/f_2$ and $F = F_1/F_2$

$$\eta = (r_1 + (r_2/\alpha))\zeta - (r_2/\alpha), \qquad (2)$$

where $\eta = (f(F - 1))/(F(\alpha + (f^2/F))$; $\zeta = (f^2/F)/(\alpha + (f^2/F))$; $\alpha = ((f^2/F)_{max} \times (f^2/F)_{min})^{0.5}$

$$F_1 = (r_1f_1^2 + f_1f_2)/(r_1f_1^2 + 2f_1f_2 + r_2f_2^2). \qquad (3)$$

Using the above determined reactivity ratios, the Skeist's model[52] (eqn (4) and (5)) was also used to predict the cumulative and instantaneous copolymer composition (F_{cumul} and F_{inst}) at any monomer conversion and to describe the possible composition drift along the chains leading to gradient copolymers.

$$\text{Conv} = 1 - (M/M_0) = 1 - [(f_1/f_1^\circ)^\alpha(f_2/f_2^\circ)^\beta\,[(f_1^\circ - \delta)/(f_1 - \delta)^\gamma], \qquad (4)$$

where M_0 and M are the initial and the instantaneous monomer concentrations, f° and f correspond to the initial and the instantaneous mole fractions in the feed and α, β, δ, and γ are defined as follows: $\alpha = r_2/(1 - r_2)$; $\beta = r_1/(1 - r_1)$; $\gamma = (1 - r_1r_2)/(1 - r_1)\,(1 - r_2)$; $\delta = (1 - r_2)/(2 - r_1 - r_2)$

$$F_{1\,cumul} = [f_1^\circ - f_1(1 - \text{conv})]/\text{conv}. \qquad (5)$$

SYNTHESIS OF P(*N*VA-*CO*-VAC) BY CMRP

A solution of alkyl–cobalt(III) initiator (PVAc$_{<4}$-Co(acac)$_2$) in CH_2Cl_2 (4.0 mL of a 0.088 M stock solution, 0.35 mmol) was taken in a flask under argon and evaporated to dryness under reduced pressure at room temperature followed by the addition of a degassed solution of *N*VA (10.4 g, 123 mmol) and VAc (11 mL, 10.3 g, 119 mmol) in dry DMF (7.6 mL). As a reference, a sample was withdrawn at the initial stage of the reaction and analyzed by ^{1}H NMR in MeOD. The reaction flask was then heated at 40 °C. After 2 h 20 min, the conversion determined by ^{1}H NMR in MeOD reached 29% and the polymerization was stopped by the addition of propanethiol (0.8 mL, 0.7 g, 9 mmol) in order to remove the cobalt complex according to a previous report.[53] The copolymer was then purified by filtration on Celite in order to remove a black residue formed upon the addition of propanethiol. The resulting solution was evaporated to dryness under reduced pressure. Finally, the copolymer was purified by precipitation in acetone followed by dialysis (membrane 3.5 kDa) against methanol for 48 h. Ultimately, the purified copolymer **A** was characterized by ^{1}H NMR and HSQC in MeOD, SEC in DMF, IR and ICP. ($M_{n,SEC\ DMF\ cal\ PS}$ = 38200 g mol^{-1}, $Đ_{SEC\ DMF\ cal\ PS}$ = 1.30, F_{NVA} = 0.72 et [Co] = 13.4 ppm).

Published in : Polymer Chemistry (2019), vol. 10, n°23, pp. 3055–3065
DOI: 10.1039/c9py00020h
Status : Postprint (Author's version)

SYNTHESIS OF P(VAM-*CO*-VA) BY ACIDIC HYDROLYSIS PROCEDURE

1 g of the above mentioned P(*N*VA-*co*-VAc) copolymer **A** (38 200 g mol^{-1}, F_{NVA} = 0.72) was dissolved in 10 mL of HCl 2 N. The resulting solution was then placed in a Parr acid digestion vessel and heated at 120 °C for 48 h. After cooling, the solution was diluted with 10 mL of water and dialyzed (membrane 8 kDa) against pure distilled water for 48 h. Finally, the P(VAm-co-VA) copolymer **B** was recovered as a powder upon lyophilisation followed by characterization *via* ^{1}H NMR and HSQC in D_2O and by FT-IR.

A similar procedure was applied for the conversion of the P(*N*VA-*co*-VA) copolymer **C** into P(VAm-*co*-VA) copolymer **D**. In this case, the reaction time was shortened to 14 h.

SYNTHESIS OF P(*N*VA-*CO*-VA) BY BASIC HYDROLYSIS PROCEDURE

1 g of P(*N*VA-*co*-VAc) copolymer **A** (38 200 g mol^{-1}, F_{NVA} = 0.72) was dissolved in 10 mL methanol containing 0.25 g of KOH. The reaction mixture was maintained under stirring at room temperature for 48 h. The solution was then diluted with 10 mL of water and dialyzed (membrane 8 kDa) against pure distilled water for 48 h. The P(*N*VA-*co*-VA) copolymer **C** was recovered as a white powder upon lyophilisation followed by characterization *via* ^{1}H NMR and HSQC in D_2O and by FT-IR.

Results and discussion

COBALT-MEDIATED RADICAL COPOLYMERIZATION OF NVA AND VAC

Before addressing the cobalt-mediated radical copolymerization of *N*VA and VAc, it is essential to recall some key mechanistic principles governing the CMRP of vinyl esters and *N*-vinyl amides (**Scheme 2**) as well as optimal conditions used for controlling their respective homopolymerization.

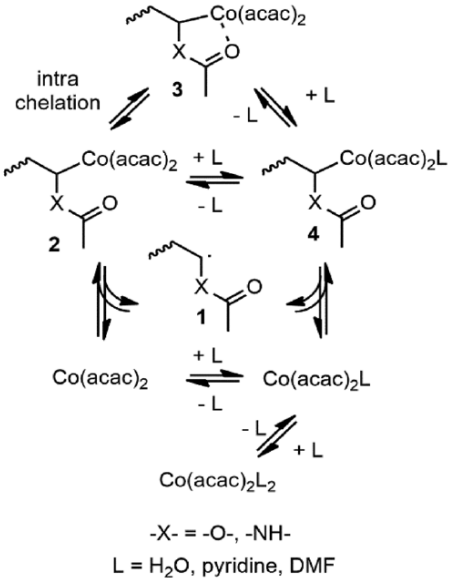

Scheme 2. Key principles of mechanism of the cobalt-mediated radical polymerization of vinyl esters and *N*-vinyl amides.

Published in : Polymer Chemistry (2019), vol. 10, n°23, pp. 3055–3065
DOI: 10.1039/c9py00020h
Status : Postprint (Author's version)

First, CMRP consists in the reversible termination of the growing radical chains **1** by a cobalt complex and the reactivation of the alkyl–cobalt dormant species 2 occurs via a thermal or photochemical treatment (**Scheme 2**). The homolytic cleavage of the Co–C bond and so the position of the equilibrium between the active **1** and dormant **2** species depend on the structures of the radical chains and of the cobalt complex. In this respect, $Co(acac)_2$ proved to be a good candidate for controlling the homopolymerization of VAc[44,45] and of *N*VA[36,37] at moderate temperatures. For example, an excellent level of control of the polymerization of VAc was achieved when carried out in bulk at 40 °C using a preformed $PVAc_{\sim 4}$-$Co(acac)_2$ species as the initiator. Under these conditions, PVAc with low dispersity ($Đ \sim 1.1$) and predictable molar mass was obtained.[45] Importantly, in the absence of coordinating molecules, this system benefits from the extra stabilization of the dormant species upon intramolecular chelation *via* the terminal ester unit of the PVAc chain **3** which displaces the equilibrium towards the dormant species.[44,54,55] Conversely, the addition of coordinating molecules in the medium competes with this intra molecular chelation leading to the dormant species **4**. Moreover, this ligand also converts the deactivating $Co(acac)_2$ species into inactive $Co(acac)_2L_2$, which ultimately shifts the equilibrium towards the active radical species.[44,54,55] The prevalence of the phenomenon largely depends on the nature of the coordinating molecules.[55] Indeed, water and pyridine are considered as strong coordinating molecules for $Co(acac)_2$ that impact much more the course of CMRP than dimethylformamide (DMF) which is regularly used as a solvent for CMRP.[37,55] These mechanistic considerations also prevail in the CMRP of *N*-vinyl amides, especially of *N*VA. Although the best control of the *N*VA polymerization was achieved using a low temperature photochemical initiating system starting from $Co(acac)_2$ associated with an azoinitiator, efficiency factors as low as 10% were recorded under these conditions.[36] Alternatively, well-defined P*N*VA ($Đ \sim 1.2$–1.4) were recently produced using $PVAc_{\sim 4}$-$Co(acac)_2$ as the initiator at 40 °C in DMF,[37] which was selected for its ability to solubilize P*N*VA and *N*VA whose melting point is equal to 51 °C. Compared to the photochemically initiated CMRP of NVA, this thermally initiated process offered higher efficiency factors ($f_{eff} \sim 0.4$).[37]

Taking into account all these aspects, preliminary assays of cobalt-mediated radical copolymerization of VAc and *N*VA were carried out at 40 °C with the $PVAc_{\sim 4}$-$Co(acac)_2$ initiator (**Scheme 3**). Because *N*VA presents a limited solubility in VAc at this temperature, we preferred a solution copolymerization process in DMF in order to cover the whole range of copolymer compositions. Three initial comonomer feeds with an *N*VA molar fraction (f°_{NVA}) ranging from 0.3 to 0.7 were considered. In terms of dilution, we started with a monomers/DMF ratio of 1/1 (g mL^{-1}). The molecular parameters (M_n and $Đ$) of the copolymer and the monomer conversion were monitored throughout the polymerization via SEC in DMF and ^{1}H NMR in MeOD, respectively. A typical ^{1}H NMR spectrum of the crude copolymerization medium is provided in **Fig. S1†**. At the end of the polymerization, the reaction was quenched by the addition of TEMPO which traps the radical chains irreversibly before purification of the copolymer *via* precipitation. The composition of the copolymer (F) was determined *via* ^{1}H NMR in MeOD by comparing of the relative intensity of signals corresponding to each comonomer unit (**Fig. S2†**). Data are reported in **Table 1**.

Published in : Polymer Chemistry (2019), vol. 10, n°23, pp. 3055–3065
DOI: 10.1039/c9py00020h
Status : Postprint (Author's version)

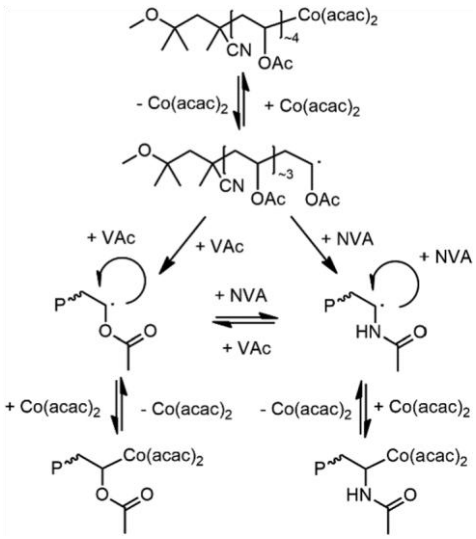

Scheme 3. Cobalt-mediated radical copolymerization of *N*VA and VAc initiated from PVAc$_{<4}$-Co(acac)$_2$.

Table 1 Cobalt-mediated radical copolymerization of *N*VA and VAc at 40 °C in DMF (1 mL g^{-1} of comonomers)

f°_{NVA} [a]	Time (h)	Conv.[a] (%)	$M_{n\ SEC}$ [b] (g mol^{-1})	$Đ$[b]	F_{NVA} [c]
0.3	1	19	11 500	1.21	
	2	23	17 100	1.25	
	4	28	21 400	1.39	
	8	38	24 500	1.58	
	13	42	26 400	1.63	0.46
0.5	1	22	19 100	1.23	
	3	36	29 000	1.42	
	5	40	31 800	1.50	
	8	46	33 000	1.61	
	11	47	32 900	1.65	0.70
0.7	0.5	26	19 300	1.25	
	1	31	25 600	1.34	
	2	41	33 200	1.44	
	3	48	38 100	1.54	
	4	52	41 300	1.63	0.81

Conditions: 40 °C, [monomer]/[PVAc$_{\sim 4}$-Co(acac)$_2$] = 500, monomers/DMF = 1/1 (m v^{-1}). [a] Determined by ^{1}H NMR in MeOD. [b] Determined by SEC in DMF/LiBr using a PS calibration. [c] Determined by ^{1}H NMR in MeOD of the isolated copolymer.

Irrespective of the initial composition of the feed, PVAc$_{<4}$Co(acac)$_2$ successfully initiated the radical copolymerization of VAc/*N*VA. Moreover, the copolymerization rate was higher when the feed was richer in *N*VA. Indeed, 40% of the monomer conversion was reached after 2 h when the *N*VA molar fraction in the feed (f°_{NVA}) was equal to 0.7, whereas 13 h was necessary to achieve the same conversion for f°_{NVA} of 0.3. This is explained by the higher propagation rate constant of *N*VA compared to VAc and by the previously observed lower bond strength of the terminal -*N*VA-Co species compared to VAc-Co.[36] Interestingly, the molar fraction of *N*VA in the copolymers (F_{NVA}) was always higher than its molar fraction in the initial feed (f°_{NVA}), indicating a preferential incorporation of *N*VA in the copolymer. This observation will be confirmed by the reactivity ratios measured in the next section. As expected for a controlled radical copolymerization, the molar masses increased with the monomer conversion. However, the dipersities tend to broaden along the polymerization and reached 1.6 at around 50% of the conversion. As an illustration, the dependence of the molecular parameters (M_n, $Đ$)

Published in : Polymer Chemistry (2019), vol. 10, n°23, pp. 3055–3065
DOI: 10.1039/c9py00020h
Status : Postprint (Author's version)

of the copolymer on the monomer conversion is plotted in **Fig. S3**. The overlay of the SEC chromatograms also showed the shift of the chromatograms towards lower elution volume (**Fig. 1**). Moreover, a tailing appeared on the higher elution volume side of the main peak, probably due to the formation of dead chains of low molar masses resulting from irreversible termination reactions. Interestingly, this loss of control seemed more critical for copolymerizations with higher VAc content, suggesting that the polymerization conditions were less favourable towards the incorporation of VAc units. This might be due to the presence of DMF that can compete with the intramolecular chelation phenomenon known to provide extra stabilization to the terminal -VAc-Co dormant chain in the absence of coordinating molecules.

Because a large amount of DMF, *i.e.* 1 mL of DMF per gram of comonomers, seemed detrimental to the control of the *N*VA/VAc copolymerizations, especially those involving high content of VAc, we decreased the volume of DMF based on the *N*VA content (1 mL of DMF per gram of *N*VA) in order to guarantee the solubility of *N*VA and to limit the possible weakening of the terminal VAc-Co(acac)$_2$ bonds. Results are presented in **Table 2**. In spite of their lower content in DMF, a molecule that favors the activation of the CMRP dormant species, copolymerizations presented in **Table 2** were faster compared to those reported in **Table 1** as a result of the more concentrated polymerization conditions. Indeed, for a stoichiometric amount of *N*VA/VAc in the initial feed, the conversion reached about 40% after only 3 h (**Table 2**, exp 2) compared to 5 h when a larger amount of DMF was used (**Table 1**, exp 2). As expected, the level of control of the copolymerization also significantly improved when adjusting the volume of DMF on the quantity of *N*VA involved in the copolymerization. For example, dispersities were lower (*Đ*∼ 1.1–1.3 until 50% of the monomer conversion) and molar masses increased regularly with the monomer conversion. The beneficial effect of the reduced DMF content in the polymerization mixture is also clear when considering the evolution of the SEC chromatograms with time (**Fig. 2**). In these experiments, the tailing attributed to the formation of dead chains was considerably attenuated.

Table 2 Cobalt-mediated radical copolymerization of *N*VA and VAc at 40 °C in DMF (1 mL g^{-1} of *N*VA)

f°_{NVA} [a]	Time (h)	Conv.[a] (%)	$M_{n\ SEC}$ [b] (g mol^{-1})	$Đ$[b]	F_{NVA} [c]
0.3	0.5	7	4800	1.10	
	1	13	7400	1.09	
	2	17	11 600	1.09	
	4	23	17 100	1.15	
	6	31	19 900	1.20	
	7.5	33	21 100	1.25	0.53
0.5	1	27	19 700	1.15	
	2	38	27 000	1.23	
	3	42	30 300	1.27	
	4	54	36 200	1.36	
	6	53	35 900	1.41	0.75
0.7	0.5	25	19 100	1.17	
	1	38	28 600	1.20	
	1.5	42	31 300	1.24	
	2	44	34 300	1.26	
	3	46	34 200	1.29	0.87

Conditions: 40 °C, [monomer]/[PVAc$_{\sim 4}$-Co(acac)$_2$] = 500, *N*VA/DMF = 1/1 (m v^{-1}). [a] Determined by ^{1}H NMR in MeOD. [b] Determined by SEC in DMF/LiBr using a PS calibration. [c] Determined by ^{1}H NMR in MeOD of the isolated copolymer.

The efficiency factors (f_{eff}) of these copolymerizations were determined by comparison of the experimental molar masses ($M_{n\ exp}$) of the copolymers measured by ^{1}H NMR and theoretical molar

Published in : Polymer Chemistry (2019), vol. 10, n°23, pp. 3055–3065
DOI: 10.1039/c9py00020h
Status : Postprint (Author's version)

masses ($M_{n\ th}$) calculated based on the monomer/initiator molar ratio and the monomer conversion. In general, the adequacy between $M_{n\ th}$ and $M_{n\ exp}$ was higher for the *N*VA/VAc copolymerization compared to the homopolymerization of *N*VA ($f_{eff} \sim 0.1–0.4$).[36,37] Indeed, the f_{eff} measured for the CMRP of *N*VA/VAc were close to unity and tended to increase with the amount of VAc in the feed (f_{eff} = 1.02, 0.93, 0.84 for f°_{NVA} = 0:3; 0:5; 0:7, respectively).

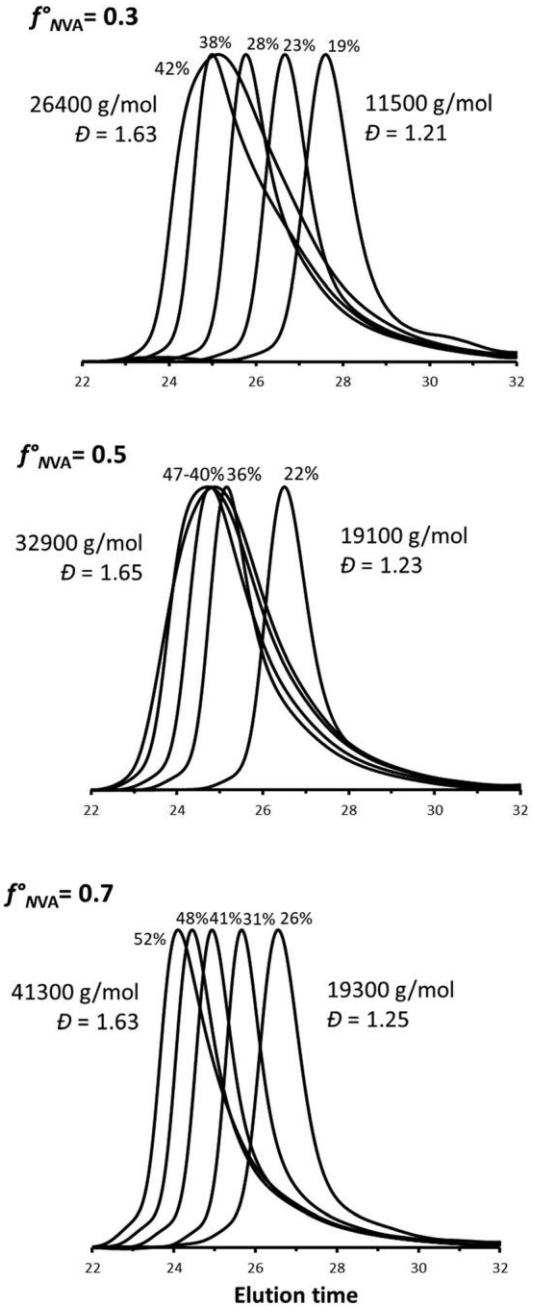

Fig. 1 Overlay of SEC chromatograms for the cobalt-mediated radical copolymerization of *N*VA and VAc at 40 °C, [monomer]/[PVAc~4Co(acac)$_2$] = 500, comonomers/DMF = 1/1 (m v^{-1}).

Published in : Polymer Chemistry (2019), vol. 10, n°23, pp. 3055–3065
DOI: 10.1039/c9py00020h
Status : Postprint (Author's version)

Again, the *N*VA content in the copolymer was higher than in the initial feed ($F_{NVA} > f^{\circ}_{NVA}$) (**Table 2**). Such a preferential incorporation of *N*VA in the copolymer goes hand in hand with a composition drift phenomenon with an increase in VAc in the feed and in the copolymer along the polymerization. This could be the reason for the slowing-down of the copolymerization occurring at around 40% conversion (**Table 2**). Indeed, in agreement with the persistent radical effect, a certain amount of $Co(acac)_2$ deactivator is formed at the early stage of the reaction to regulate the copolymerization integrating predominantly *N*VA units. However, this amount of $Co(acac)_2$ might be too elevated later in the reaction when the VAc content in the feed and in the copolymer increases which could slow down the polymerization. Prediction of the poly(*N*VA-*co*-VAc) composition and evaluation of this composition drift requires proper determination of the reactivity ratios.

CONTROL OF THE P(NVA-CO-VAC) COMPOSITION AND COMONOMER DISTRIBUTION

In order to predict the composition of the poly(*N*VA-*co*-VAc) copolymers produced by CMRP and get insight into the distribution of the *N*VA and VAc units along their backbone, we determined the reactivity ratios for the copolymerization of these monomers *via* CMRP. For that purpose, a series of copolymerizations were initiated at 40 °C by $PVAc_{\sim 4}$-$Co(acac)_2$ in DMF for different initial feed compositions (f°_{NVA} ranging from 0.1 to 0.9). Polymerizations were stopped at a low monomer conversion in order to prevent significant composition drift which would alter the accuracy of the reactivity ratio values. Typically, we used a comonomer/initiator molar ratio as high as 700 leading to copolymers with decent molar masses at a low conversion, which facilitates their recovery and purification. The copolymers were purified by dialysis against methanol before determination of the composition via ^{1}H NMR in MeOD by comparing the relative intensity of signals characteristic of each comonomer unit. Based on the data provided in **Table S1†**, the cumulative molar fraction of *N*VA in the P(*N*VA-*co*-VAc) copolymer (F_{NVA}) was plotted as a function of its molar fraction in the feed (f_{NVA}) (**Fig. 3**). Then, the *N*VA/Vac reactivity ratios were determined by Fineman–Ross[48] (***FR***, **Fig. S4†**) and Kelen–Tüdos[49] (***KT***, **Fig. S5†**) linearization methods as well as by least squares fitting curve according to the Mayo–Lewis equation[50,51] (***ML***, **Fig. 3**). As illustrated in **Table 3**, values obtained by these approaches were highly consistent. The average values for $r_{NVA/VAc}$ and $r_{VAc/NVA}$ were equal to 2.2 and 0.35, respectively, which confirmed the preferential incorporation of *N*VA within the P(*N*VA-*co*-VAc) copolymers and the occurrence of a composition drift along the copolymerization. By using the Skeist's model,[52] we predicted such a compositional drift along the P(*N*VA-*co*-VAc) backbone as a function of the degree of completion of the polymerization (**Fig. 4**). This also provides a clear idea of the distribution of the comonomers within the copolymer. **Fig. 4** represents the evolution of the cumulative ($F_{NVA\ cumul}$) and instantaneous ($F_{NVA\ Inst}$) molar fractions of *N*VA in the P(*N*VA-*co*-VAc) copolymer as a function of the overall molar monomer conversion for different initial comonomer feed ratios (f°_{NVA}). As a confirmation of the validity of this model, the compositions of the P(*N*VA-*co*-VAc) copolymers presented in **Table 1** were consistent with the predictive cumulative molar fraction of *N*VA shown in **Fig. 4**. However, we observed a discrepancy of few percent between the compositions predicted in **Fig. 4** and the composition of copolymers in **Table 2**. In the latter case, DMF was adjusted based on the *N*VA content only, so the comonomers/DMF ratio was varied, which might be the reason

Published in : Polymer Chemistry (2019), vol. 10, n°23, pp. 3055–3065
DOI: 10.1039/c9py00020h
Status : Postprint (Author's version)

for the slight deviation from the predictive model. Typically, the graphs in **Fig. 4** show a significant change of the composition of the copolymer with the conversion. In particular, the $F_{NVA\ Inst}$ drastically drops above 40–50% of the conversion leading to a gradient of composition which becomes richer in VAc as the conversion increases. This observation is in line with our hypothesis suggesting that the progressive exchange of terminal *N*VA-Co species for VAc-Co units may cause the slowing down, and ultimately the inhibition, of the CMRP of *N*VA/VAc. Overall, this model provides a precise picture of the compositional distribution of the P(*N*VA-*co*-VAc) copolymers used as precursors of P(VAm-*co*-VA)s.

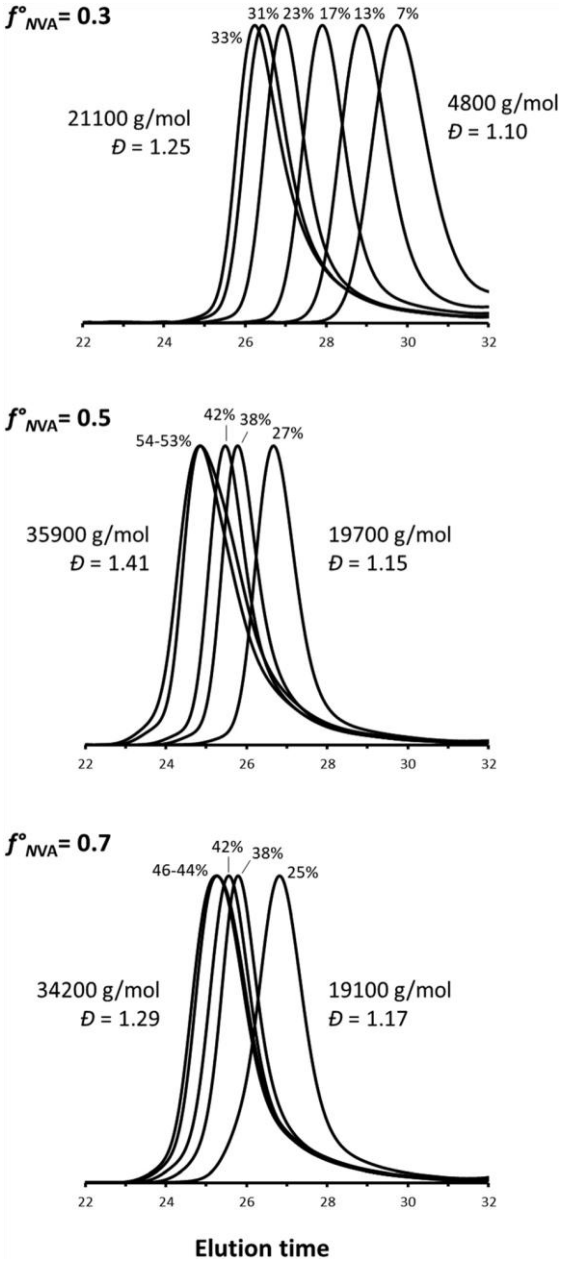

Fig. 2 Overlay of SEC chromatograms for the cobalt-mediated radical polymerization of *N*VA and VAc at 40 °C, [monomer]/[PVAc~4-Co(acac)$_2$] = 500, *N*VA/DMF = 1/1 (m v^{-1}).

Published in : Polymer Chemistry (2019), vol. 10, n°23, pp. 3055–3065
DOI: 10.1039/c9py00020h
Status : Postprint (Author's version)

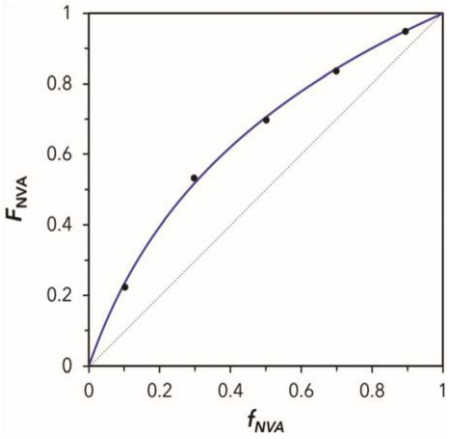

Fig. 3 Relationship between the molar fraction of *N*VA in the copolymer (F_{NVA}) and in the feed (f_{NVA}) for the cobalt-mediated radical copolymerization of *N*VA and VAc at 40 °C in DMF. The blue line represents the fitting curves obtained by the least square method according to the Mayo–Lewis equation.

Table 3 Reactivity ratios determined for the CMRP of *N*VA/VAc

Method	$r_{NVA/VAc}$	$r_{VAc/NVA}$
Fineman–Ross	2.20	0.36
Kelen–Tüdos	2.17	0.34
Mayo–Lewis	2.22	0.34

Determined based on the data collected from **Table S1**. For more details, see **Experimental section**.

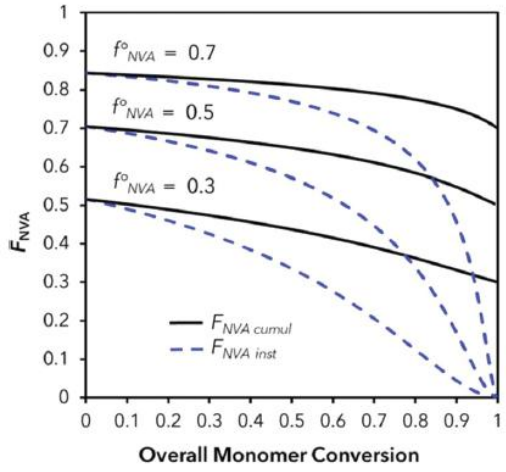

Fig. 4 Dependence of the cumulative ($F_{NVA\ cumul}$) and instantaneous ($F_{NVA\ Inst}$) molar fractions of *N*VA in the P(*N*VA-*co*-VAc) copolymer on the overall molar monomer conversion during the *N*VA/VAc copolymerization by CMRP starting from different initial comonomer feed ratios (f°_{NVA}). Compositions are calculated based on the Skeist's model.

SYNTHESIS OF VINYL AMINE/VINYL ALCOHOL BASED COPOLYMERS

After developing the controlled synthesis of the P(*N*VA-*co*-VAc) copolymers, we examined their conversion into P(VAm-*co*-VA)s. It may be recalled that PVA is produced at a large scale via saponification of the ester moieties in alcoholic media in the presence of sodium or potassium hydroxide.[1,2,35,56] The preparation of PVA can also be achieved upon the treatment of PVAc with sulfuric acid.[57,58] On the other hand, PVAm is commonly produced upon basic or acidic treatments of P*N*VF.[24–

Published in : Polymer Chemistry (2019), vol. 10, n°23, pp. 3055–3065
DOI: 10.1039/c9py00020h
Status : Postprint (Author's version)

[26] However, the hydrolysis of the amide moieties of P*N*VA is more challenging and requires drastic conditions. For example, prolonged treatment of P*N*VA at 80 °C in concentrated NaOH solution did not lead to PVAm.[24] In contrast, P*N*VA can be converted into PVAm under acidic conditions by reaction with HCl at elevated temperatures.[14,27–29,36] As an illustration, the conversion of amides into amines reached up to 94% upon treatment of P*N*VA with HCl at 120 °C.[36] This procedure was notably applied for designing well-defined PVAms *via* sequential CMRP of *N*VA and acidic hydrolysis of P*N*VA.[36]

In the light of these considerations, various hydrolysis procedures were tested on the P(*N*VA-*co*-VAc) copolymer **A** ($M_{n\,SEC}$ = 38 200 g mol^{-1}, $Đ$ = 1.30, F_{NVA} = 0.72) prepared by CMRP (**Scheme 4**). As described elsewhere,[53] at the end of the controlled copolymerization, propanethiol was added to the reaction mixture for substituting the cobalt complex by a hydrogen atom at the copolymer chain-end in order to prevent any stability issue of the terminal function under acidic or basic conditions. Based on the inductively coupled plasma (ICP) analysis, this treatment reduced the residual cobalt content from 2880 ppm to 13 ppm, *i.e.* a reduction of 99.5%. Reactions applied to copolymer **A** for its conversion into amine- and alcohol-containing copolymers are summarized in **Scheme 4**.

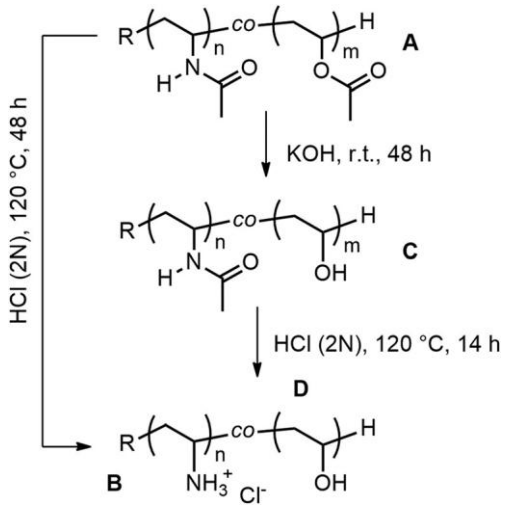

Scheme 4 General strategy for the synthesis of P(VAm-*co*-VA) and P(*N*VA-*co*-VA) via acidic and basic hydrolysis of P(*N*VA-*co*-VAc).

Inspired by the above mentioned procedures leading to high levels of hydrolysis of PVAc and P*N*VA, P(*N*VA-*co*-VAc) was first heated at 120 °C in HCl (2 N) for 48 h. Expectedly, the successful conversion of P(*N*VA-*co*-VAc) **A** into the corresponding P(VAm-*co*-VA) **B** was confirmed by infrared (**Fig. S6†**) and NMR (**Fig. S7†**) spectroscopies. Indeed, IR spectra show the disappearance of characteristic signals of the esters of the VAc units (C=O ester) at 1250 cm^{-1} and the appearance of a large band at 3300 cm^{-1} typical of the hydroxyl group of the VAm units (**Fig. S6†**). In addition, signals relative to the *N*VA units (C=O amide at 1670 cm^{-1} and N–H amide at 1560 cm^{-1}) disappeared whereas a peak corresponding to the protonated amine appeared at 2800 cm^{-1}. We also observed drastic changes in the ^{1}H NMR (**Fig. S7†**) and HSQC (**Fig. 5**A and B) spectra in D_2O after hydrolysis. Indeed, signals corresponding to the hydrogen of the methyl groups of the *N*VA (**c**) and VAc (**f**) units of the copolymer disappeared. Moreover, the signal at 4.8 ppm corresponding to the methine protons of the VAc units (d) was shifted upon hydrolysis at 4 ppm (**d'**) which is typical of VA units. Another confirmation of the change in the polymer structure upon hydrolysis is given by the thermogravimetric analysis (TGA),which exhibits a

Published in : Polymer Chemistry (2019), vol. 10, n°23, pp. 3055–3065
DOI: 10.1039/c9py00020h
Status : Postprint (Author's version)

significant decrease of the onset temperature of the thermal degradation of the copolymer before (copolymer **A**) and after (copolymer **B**) the acidic hydrolysis, i.e. from 269 °C to 159 °C (**Fig. S8**). Overall, this acidic treatment gave access to the desired P(VAm-*co*-VA) which was fully soluble in water over a wide range pH values (pH tested from 1 to 13).

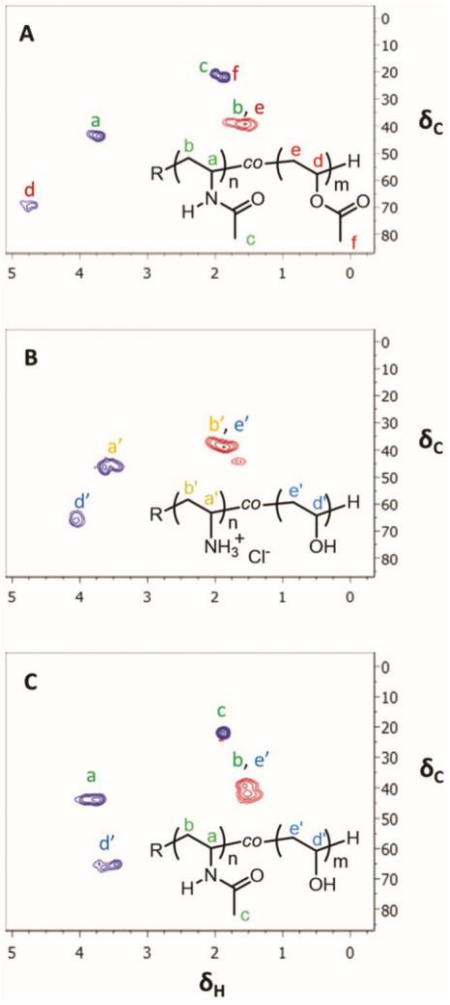

Fig. 5 HSQC spectra in D_2O of the P(*N*VA-*co*-VAc) copolymer **A** prepared by CMRP and of the corresponding P(VAm-*co*-VA) copolymer **B** and P(*N*VA-*co*-VA) copolymer **C** produced via acidic and basic treatment of **A**, respectively.

In order to extend the range of materials that can be achieved from P(*N*VA-*co*-VAc) **A**, we considered its basic treatment under mild conditions (KOH, room temperature, 14 h) expecting the selective hydrolysis of the ester groups and the production of the water soluble P(*N*VA-*co*-VA) copolymer **C**. The IR spectrum of the copolymer after such a treatment proved the disappearance of the ester functions, whereas amides remained intact (**Fig. S6†**). As a confirmation, the HSQC peak corresponding to the methyl group of the VAc units (**f**) disappeared contrary to those of the *N*VA units (**c** at 1.9 ppm δ_H/22 ppm δ_C) (compare **Fig. 5**A and C). Moreover, the shift of the methine hydrogen of the VAc units (from 5 ppm d to 3.7 ppm **d'**) is another confirmation of the complete hydrolysis of the ester moieties. In addition, the TGA analysis carried out on the P(*N*VA-*co*-VA) copolymer revealed an onset temperature of 306 °C (**Fig. S8†**). This strategy thus gives access to unprecedented hydrosoluble P(*N*VA-*co*-VA) copolymer **C**. Finally, the amide functions of the copolymer P(*N*VA-*co*-VA) **C** can be hydrolyzed

Published in : Polymer Chemistry (2019), vol. 10, n°23, pp. 3055–3065
DOI: 10.1039/c9py00020h
Status : Postprint (Author's version)

through treatment with HCl (2 N) at 120 °C leading to the P(VAm-*co*-VA) copolymer **D** which exhibits similar characteristics to those of **B** as confirmed by IR and HSQC spectra in D_2O (**Fig. S9†** and **S10†**).

Conclusions

Combining both vinyl amine and vinyl alcohol within a copolymer represents an attractive approach to modulate the properties of the parent homopolymers, *i.e.* poly(vinyl alcohol) and poly(vinyl amine). So far, the synthesis of such P(VAm-*co*-VA) copolymers was achieved *via* free radical copolymerization, that is to say, with poor control of the molar mass, architecture and composition but also with very limited macromolecular engineering possibilities. Here, we described for the first time a straightforward strategy for the precision design of P(VAm-*co*-VA). This approach consists of a two-step process based on cobalt-mediated radical copolymerization of *N*-vinyl acetamide and vinyl acetate followed by hydrolysis of the pendant amide and ester functions.

The controlled copolymerization of *N*VA and VAc was achieved using $Co(acac)_2$ as a mediator after optimization of the experimental conditions. We notably demonstrated that dimethylformamide is a solvent of choice provided that its concentration is properly adjusted. Indeed, the solubilisation of *N*VA requires a sufficient amount of DMF, but the latter interferes with the control of the CMRP of VAc. This is probably due to the fact that DMF competes the intramolecular chelation of the cobalt by the ester function of the last monomer units which provides extra stabilization to the terminal P-(VAc)-$Co(acac)_2$ dormant species. Overall, the best level of control of the molecular parameters was achieved by adjusting the amount of DMF in accordance with the *N*VA content in the comonomer feed. A series of P(*N*VA-*co*-VAc) copolymers with specific molar mass, low to moderate dispersity ($Đ \sim$ 1.1–1.3) and various compositions were successfully prepared under these conditions. Interestingly, much better efficiency factors ($f_{eff} \sim$ 0.85–1) were observed for the cobalt-mediated radical copolymerization of *N*VA and VAc compared to those reported for the homopolymerization of *N*VA via CMRP ($f_{eff} \sim$ 0.1–0.4). For the first time, we measured the reactivity ratios for the *N*VA/VAc copolymerization. Three different methods, i.e. the Fineman– Ross method, the Kelen–Tüdos method and the nonlinear approach, were considered and provided very similar values (r_{NVA} = 2.2, r_{VAc} = 0.35). The latter emphasized the preferential incorporation of the *N*VA in the copolymer, and the composition drift was evaluated by the Skeist's model. With these models in hand, we have now a clear view of the distribution of the comonomers along the P(*N*VA-*co*-VAc) copolymers.

Next, the conversion of these poly(*N*-vinyl acetamide-*co*-vinyl acetate)s into their vinyl amine- and vinyl alcohol-based counterparts was performed *via* hydrolysis treatments. The deprotected poly(VAm-*co*-VA) copolymers were produced via high temperature acidic hydrolysis of the poly(*N*VA-*co*-VAc) precursors, whereas selective hydrolysis of the esters was achieved under basic conditions leading for the first time to poly(*N*VA-*co*-VA)s with controlled molecular parameters, composition and comonomer distribution. Note that the controlled character of the *N*VA/VAc copolymerization also opens several macromolecular engineering opportunities like the incorporation of P(*N*VA-*co*-VAc), P(*N*VA-*co*-VA) or P(VAm-*co*-VA) sequences within complex architectures.

Published in : Polymer Chemistry (2019), vol. 10, n°23, pp. 3055–3065
DOI: 10.1039/c9py00020h
Status : Postprint (Author's version)

To conclude, we developed a strategy based on CMRP for the precision design of vinyl amine- and vinyl alcohol-based copolymers which offer prospect of fine-tuning the properties of this important class of copolymers. Indeed, a plethora of novel derivatives from amine-rich to hydroxyl-rich copolymers could arise from this RDRP route. While further investigation and characterization are necessary to establish the full potential of these sequences, the present method of synthesis represents a major step forward in the design of VAm- and VA-containing materials that are capable of outperforming PVA and PVAm homopolymers in some applications and in future.

Supplementary Information†

Table S1. Data used for the determination of the reactivity ratios for the CMRP of *N*VA and VAc.

Entry	Feed composition		Time	Conv [a]	Copolymer composition [b]	
	f°_{NVA}	f°_{VAc}	(min)	(%)	F_{NVA}	F_{VAc}
1	0.10	0.90	85	17	0.21	0.79
2	0.30	0.70	60	10	0.54	0.47
3	0.50	0.50	20	1	0.70	0.30
4	0.70	0.30	13	11	0.84	0.16
5	0.89	0.11	3	32 [c]	0.94	0.06

Conditions: 40 °C ; [Comonomers]/[$PVAc_{<4}$-$Co(acac)_2$] = 700 ; comonomers/DMF = 1.4/1 m/v.[a] Determined by ^{1}H NMR in MeOD (see **Figure S1**). [b] Determined by ^{1}H NMR in MeOD after purification of the copolymer by precipitation followed by dialysis in methanol. [c] The conversion was higher in this case due to a very fast polymerization when copolymerization with high *N*VA content is used. Nevertheless, as predicted by the Skeist's model, the composition drift is rather limited at this conversion and the value remains valid (see F_{cumul} in **Figure 4**).

Published in : Polymer Chemistry (2019), vol. 10, n°23, pp. 3055–3065
DOI: 10.1039/c9py00020h
Status : Postprint (Author's version)

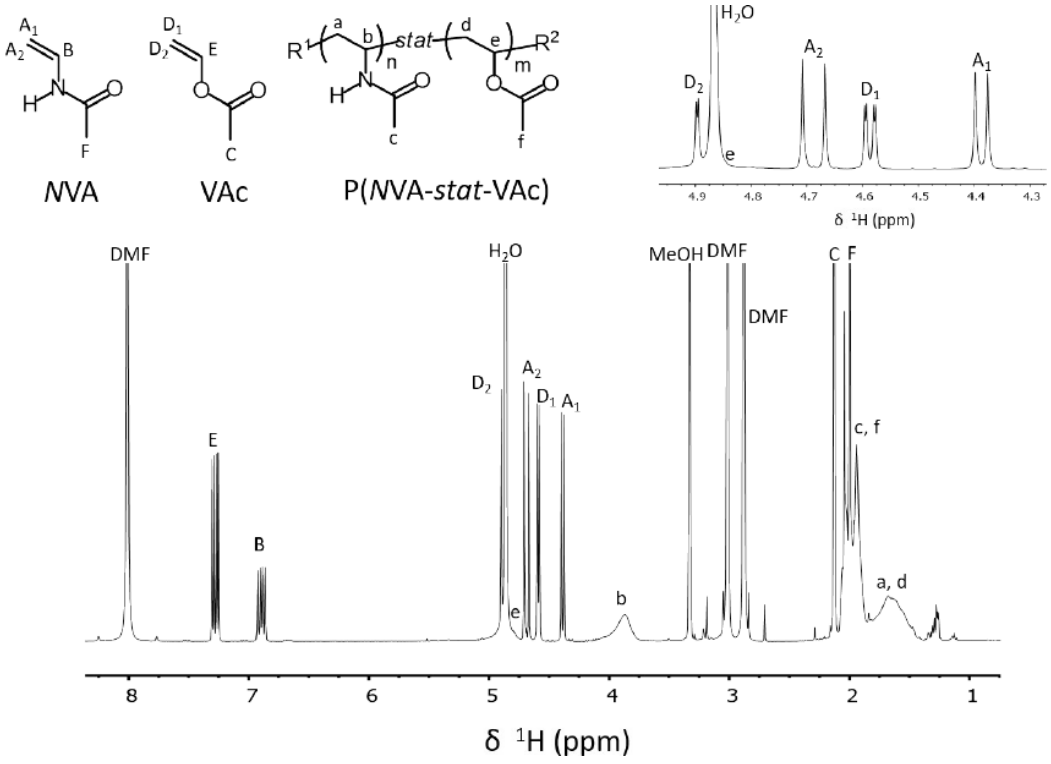

Fig S1. Typical ^{1}H NMR spectrum in MeOD of the reaction mixture of the cobalt-mediated radical copolymerization of *N*VA/VAc. Conditions: [*N*VA]/[VAc]/[RCo(acac$_2$)] = 250/250/1 ; 1 g of comonomers/mL of DMF, 40 °C, 11 h, overall conv = 47 %. Overall conversion (%) = [[[$\int_{2.2\text{-}1.4\ ppm} - 3\int_{4.6\ ppm} - 3\int_{4.4\ ppm}$ ppm]/5] / [[[$\int_{2.2\text{-}1.4\ ppm} - 3\int_{4.6\ ppm} - 3\int_{4.4\ ppm}$ ppm]/5]+ $\int_{4.6\ ppm} + \int$4.4 ppm]]×100

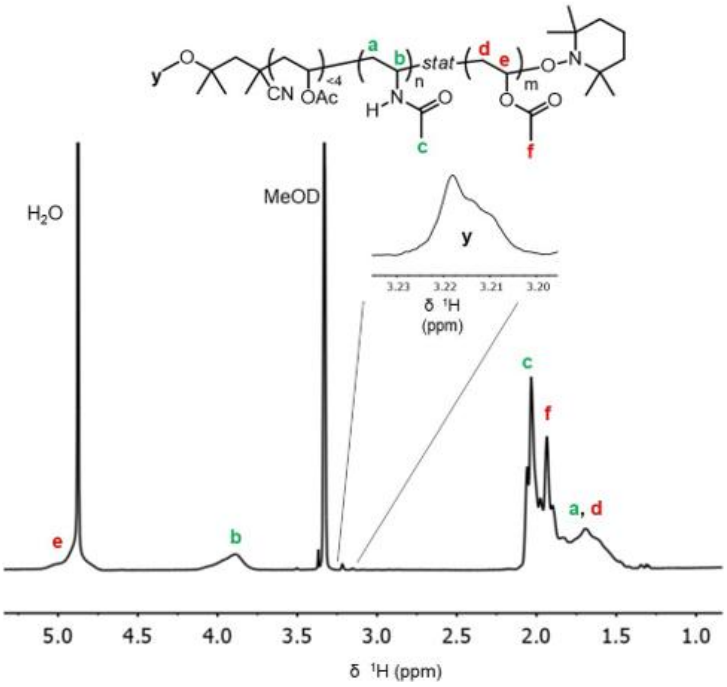

Fig S2. Typical ^{1}H NMR analysis of a P(*N*VA-*co*-VAc) copolymer prepared by cobalt-mediated radical copolymerization of *N*VA/VAc. Conditions: [*N*VA]/[VAc]/[RCo(acac$_2$)] = 150/350/1; 1 g of comonomers/mL of DMF, 40 °C, 13 h, conversion = 42 %. (See **Table 1**, f°_{NVA} = 0.3). F_{NVA} = 0.46. It was determined by comparing the intensity of signal **b** at 3.8 ppm corresponding to

Published in : Polymer Chemistry (2019), vol. 10, n°23, pp. 3055–3065
DOI: 10.1039/c9py00020h
Status : Postprint (Author's version)

the methine proton of the *N*VA units with signals between 2.3 and 1.4 ppm corresponding to the methyl and methylene groups of *N*VA and VAc units in the copolymer. ($F_{NVA} = \int_{4.2\text{-}3.6\ ppm} / [\int_{2.3\text{-}1.4\ ppm}/5]$)

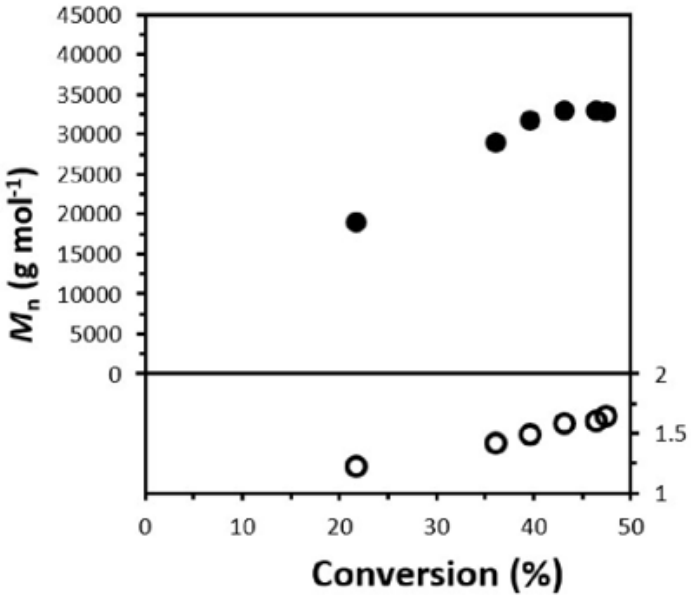

Fig S3. Dependence of the molar mass ($M_{n\ SEC\ DMF\ CAL\ PS}$, full symbols) and dispersity ($Đ$, empty symbols) on monomer conversion (determined by ^{1}H NMR in MeOD) for the cobalt-mediated radical copolymerization of *N*VA and VAc. Conditions: [Monomer]/[R-Co] = 500; [*N*VA]/[VAc]/[PVAc$_{<4}$-Co(acac)$_2$] = 250/250/1; 1 g of comonomers/ mL of DMF, 40 °C. (see **Table 1**, $f°_{NVA} = 0.5$)

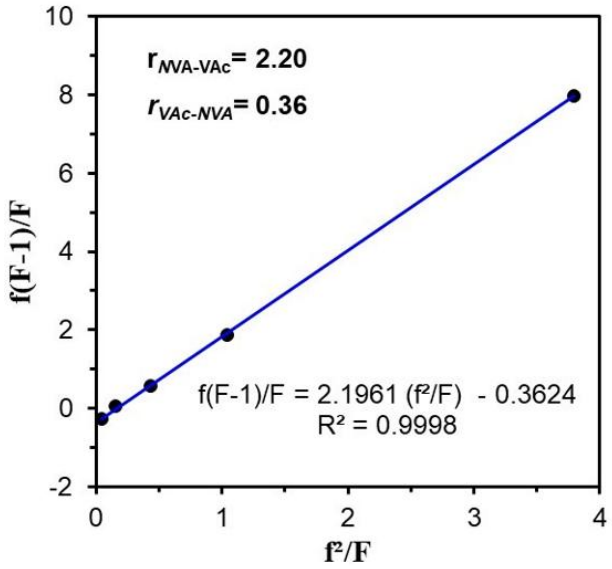

Fig S4. Fineman-Ross plot for the cobalt-mediated radical copolymerization of *N*VA and VAc in DMF at 40 °C in DMF. Experimental conditions and data are presented in **Table S1**.

Published in : Polymer Chemistry (2019), vol. 10, n°23, pp. 3055–3065
DOI: 10.1039/c9py00020h
Status : Postprint (Author's version)

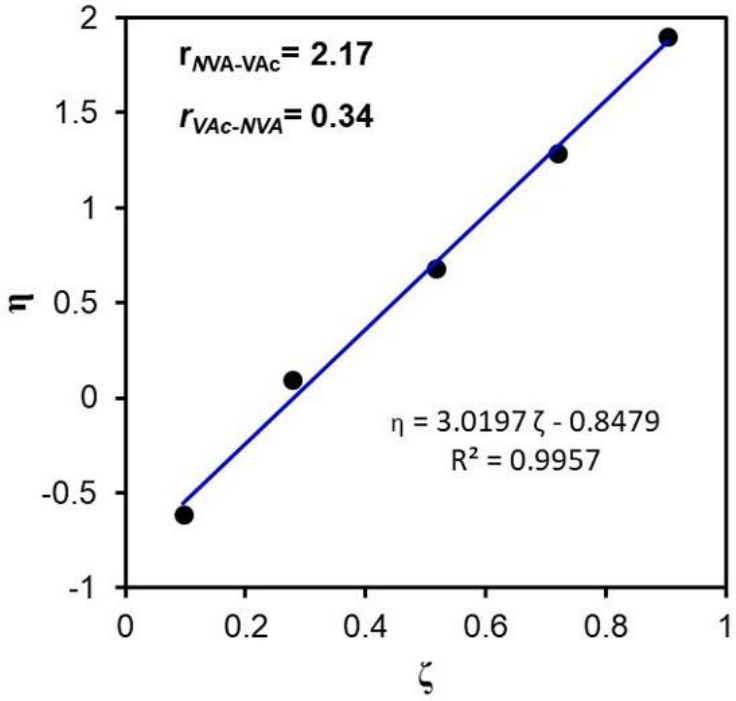

Fig S5. Kelen-Tudos plot for the cobalt-mediated radical copolymerization of *N*VA and VAc in DMF at 40 °C in DMF. Experimental conditions and data are presented in **Table S1**.

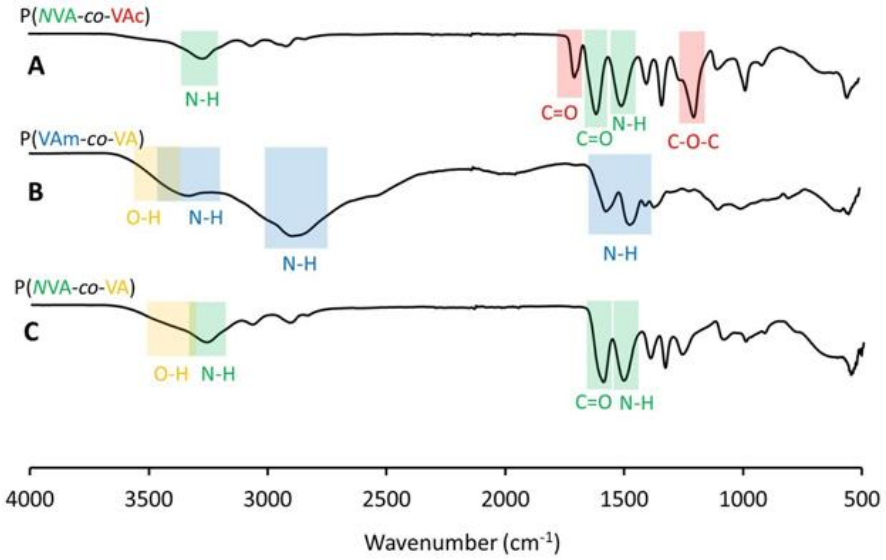

Fig S6. Infrared spectra of the P(*N*VA-*co*-VAc) copolymer (**A**) prepared by CMRP and the corresponding P(VAm-*co*-VA) (**B**) and P(*N*VA-*co*-VA) (**C**) copolymers produced via total and selective hydrolysis of (**A**), respectively.

Published in : Polymer Chemistry (2019), vol. 10, n°23, pp. 3055–3065
DOI: 10.1039/c9py00020h
Status : Postprint (Author's version)

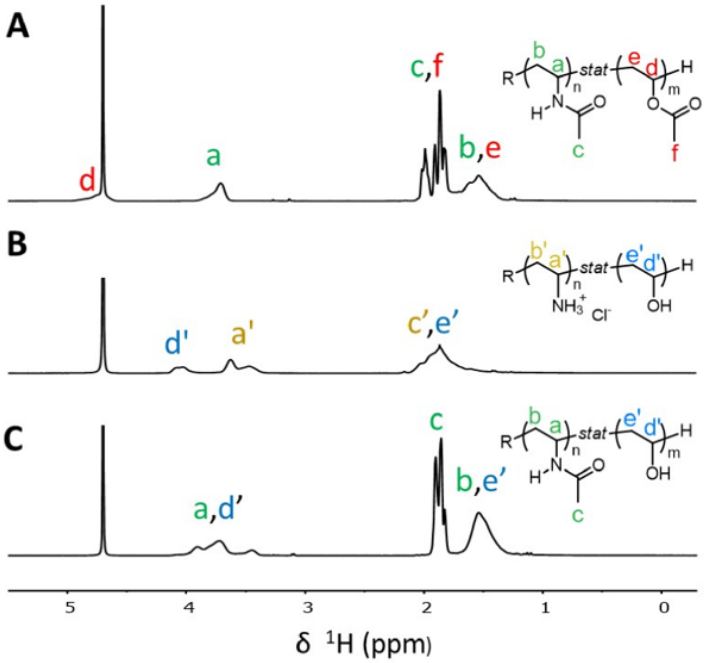

Fig S7. ^{1}H NMR spectra in D_2O of the P(*N*VA-*co*-VAc) copolymer (**A**) prepared by CMRP and the corresponding P(VAm-*co*-VA) (**B**) and P(*N*VA-*co*-VA) (**C**) copolymers produced via total and selective hydrolysis of (**A**), respectively.

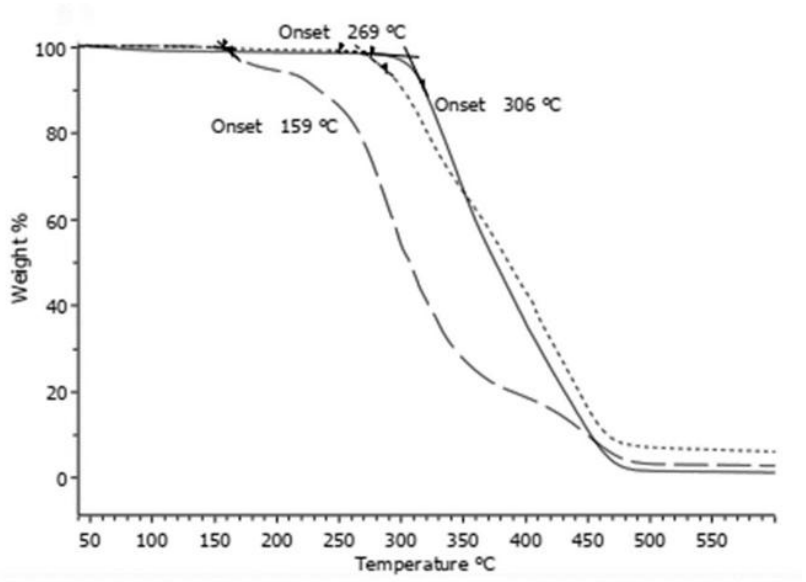

Fig S8. Thermogravimetric analysis of the P(*N*VA-*co*-VAc) copolymer **A** (----) prepared by CMRP and the corresponding P(VAm-*co*-VA) **B** (——) and P(*N*VA-*co*-VA) **C** (——) copolymers produced via total and selective hydrolysis of (**A**), respectively.

Published in : Polymer Chemistry (2019), vol. 10, n°23, pp. 3055–3065
DOI: 10.1039/c9py00020h
Status : Postprint (Author's version)

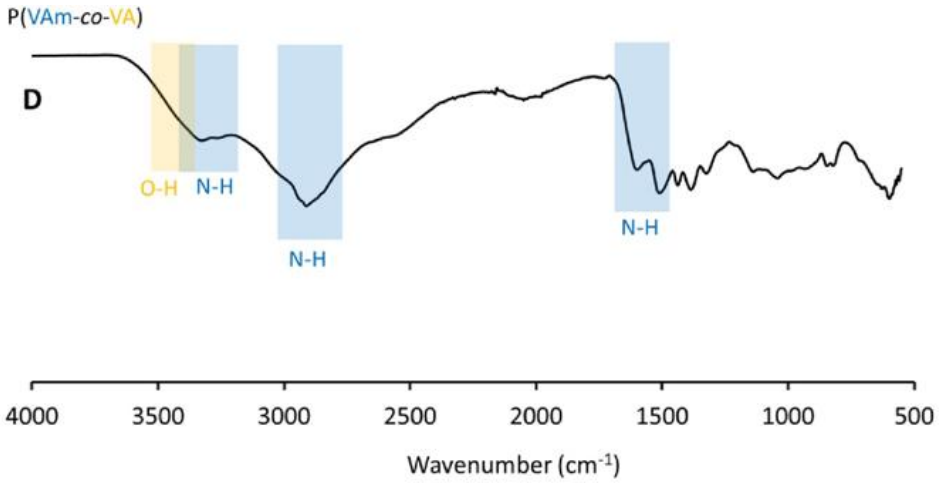

Fig S9. IR spectrum of the P(VAm-*co*-VA) (**D**) obtained via hydrolysis of P(*N*VA-*co*-VA) copolymer (**B**) through treatment with HCl (2N) at 120 °C for 14 h.

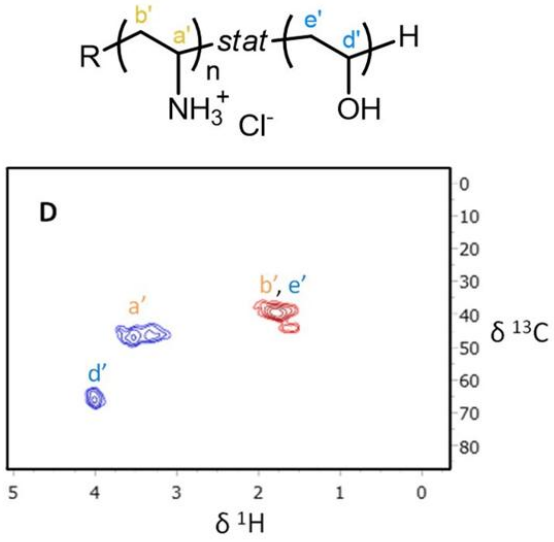

Fig S10. HSQC spectrum in D_2O of the P(VAm-*co*-VA) (**D**) obtained via hydrolysis of P(*N*VA-*co*-VA) copolymer (**B**) through treatment with HCl (2N) at 120 °C.

Conflicts of interest

There are no conflicts to declare.

Published in : Polymer Chemistry (2019), vol. 10, n°23, pp. 3055–3065
DOI: 10.1039/c9py00020h
Status : Postprint (Author's version)

Acknowledgements

The authors are grateful to the Belgian National Funds for Scientific Research (F.R.S.-FNRS) in Belgium for their financial support. P.S. and A.D. are FNRS PhD fellow and FNRS Research Associate, respectively.

Notes and references

1 S. Moulay, *Polym.-Plast. Technol. Eng.*, 2015, 54, 1289–1319.
2 E. Chiellini, A. Corti, S. D. Antone and R. Solaro, *Prog. Polym. Sci.*, 2003, 28, 963–1014.
3 S. Muppalaneni and H. Omidian, *J. Dev. Drugs*, 2013, 2, 1–5.
4 R. Pelton, *Langmuir*, 2014, 30, 15373–15382.
5 5 S. Yuan, Z. Wang, Z. Qiao, M. Wang, J. Wang and S. Wang, *J. Membr. Sci.*, 2011, 378, 425–437.
6 6 P. Li, Z. Wang, Y. Liu, S. Zhao, J. Wang and S. Wang, *J. Membr. Sci.*, 2015, 476, 243–255.
7 C. Geffroy, M. Labeau, K. Wong, B. Cabane and M. Cohen Stuart, *Colloids Surf.*, A, 2000, 172, 47–56.
8 T. J. Kim, L. I. Baoan and M. B. Hägg, *J. Polym. Sci., Part B: Polym. Phys.*, 2004, 42, 4326–4336.
9 A. Toutianoush, A. El-Hashani, J. Schnepf and B. Tieke, *Appl. Surf. Sci.*, 2005, 246, 430–436.
10 Q. Chen and L. Zhu, *Appl. Mech. Mater.*, 2012, 130–134, 1507–1510.
11 Y. Huang, D. Wu, X. Wang, W. Huang, D. Lawless and X. Feng, *Sep. Purif. Technol.*, 2016, 158, 124–136.
12 L. Robeson and T. Pickering, *US*, 005380403A, 1995.
13 M. A. Wolfert, P. R. Dash, O. Nazarova, D. Oupicky, L. W. Seymour, S. Smart, J. Strohalm and K. Ulbrich, *Bioconjugate Chem.*, 1999, 10, 993–1004.
14 M. Dréan, A. Debuigne, C. Jérôme, C. Goncalves, P. Midoux, J. Rieger and P. Guégan, *Biomacromolecules*, 2017, 18, 440–451.
15 R. K. Pinschmidt, *J. Polym. Sci., Part A: Polym. Chem.*, 2010, 48, 2257–2283.
16 H. Anany, W. Chen, R. Pelton and M. W. Griffiths, *Appl. Environ. Microbiol.*, 2011, 77, 6379–6387.
17 N. B. Holland, Z. Xu, K. Vacheethasanee and R. E. Marchant, *Macromolecules*, 2001, 34, 6424–6430.
18 S. M. Zakir Hossain, R. E. Luckham, A. M. Smith, J. M. Lebert, L. M. Davies, R. H. Pelton, C. D. M. Filipe and J. D. Brennan, *Anal. Chem.*, 2009, 81, 5474–5483.
19 S. Noel, B. Liberelle, A. Yogi, M. J. Moreno, M. N. Bureau, L. Robitaille and G. De Crescenzo, *J. Mater. Chem. B*, 2013, 1, 230–238.
20 W. Chen, C. Lu and R. Pelton, *Biomacromolecules*, 2006, 7, 701–702.
21 J. L. DiFlavio, R. Pelton, M. Leduc, S. Champ, M. Essig and T. Frechen, *Cellulose*, 2007, 14, 257–268.
22 B. M. Novak and A. K. Cederstav, *J. Macromol. Sci., Part A: Pure Appl.Chem.*, 1997, 34, 1815–1825.
23 B. M. Novak and J. T. Cafmeyer, *J. Am. Chem. Soc.*, 2001, 123, 11083–11084.
24 R. K. Pinschmidt, W. L. Renz, W. E. Carroll, K. Yacoub, J. Drescher, A. F. Nordquist and N. Chen, *J. Macromol. Sci., Part A: Pure Appl. Chem.*, 1997, 34, 1885–1905.

Published in : Polymer Chemistry (2019), vol. 10, n°23, pp. 3055–3065
DOI: 10.1039/c9py00020h
Status : Postprint (Author's version)

25 K. Yamamoto, Y. Imamura, E. Nagatomo, T. Serizawa, Y. Muraoka and M. Akashi, *J. Appl. Polym. Sci.*, 2003, 89, 1277–1283.
26 L. Gu, S. Zhu and A. N. Hrymak, *J. Appl. Polym. Sci.*, 2002, 86, 3412–3419.
27 M. Akashi, S. Nakano and A. Kishida, *J. Polym. Sci., Part A: Polym. Chem.*, 1996, 34, 301–303.
28 M. Akashi, S. Saihata, E. Yashima, S. Sugita and K. Marumo, *J. Polym. Sci., Part A: Polym. Chem.*, 1993, 31, 1153–1160.
29 M. Dréan, P. Guégan, C. Jérôme, J. Rieger and A. Debuigne, *Polym. Chem.*, 2016, 7, 69–78.
30 D. D. Reynolds and W. O. Kenyon, *J. Am. Chem. Soc.*, 1947, 69, 911–915.
31 R. K. Pinschmidt and T.-W. Lai, *EP*, 0339371A2, 1989.
32 32 P. Shu and K. D. Schmitt, *Colloids Surf., A*, 1996, 7757, 273– 285.
33 A. Debuigne, J. Warnant, R. Jerome, I. Voets, A. de Keizer, M. A. Cohen Stuart and C. Detrembleur, *Macromolecules*, 2008, 41, 2353–2360.
34 A. Debuigne, N. Willet, R. Jérôme and C. Detrembleur, *Macromolecules*, 2007, 40, 7111–7118.
35 M. H. Stenzel, T. P. Davis and C. Barner-kowollik, *Chem. Commun.*, 2004, 1546–1547.
36 M. Dréan, P. Guégan, C. Detrembleur, C. Jérôme, J. Rieger and A. Debuigne, *Macromolecules*, 2016, 49, 4817–4827.
37 P. Stiernet, M. Dréan, C. Jérôme, P. Midoux, P. Guégan, J. Rieger and A. Debuigne, *ACS Symp. Ser.*, 2018, 1284, 17–349.
38 Y. Maki, H. Mori and T. Endo, *Macromol. Chem. Phys.*, 2007, 208, 2589–2599.
39 X. Liang, V. Kozlovskaya, C. P. Cox, Y. Wang, M. Saeed and E. Kharlampieva, *J. Polym. Sci., Part A: Polym. Chem.*, 2014, 2725–2737.
40 A. Debuigne, C. Jerome and C. Detrembleur, *Polymer*, 2017, 115, 285–307.
41 R. Poli, Chem. – Eur. J., 2015, 21, 6988–7001. 42 M. Hurtgen, C. Detrembleur, C. Jérôme and A. Debuigne, *Polym. Rev.*, 2011, 51, 188–213.
43 A. Debuigne, J.-R. Caille and R. Jerome, *Angew. Chem., Int. Ed.*, 2005, 44, 1101–1104.
44 A. Debuigne, Y. Champouret, R. Jérôme, R. Poli and C. Detrembleur, *Chem. – Eur. J.*, 2008, 14, 4046–4059.
45 A. N. Morin, C. Detrembleur, C. Jérôme, P. De Tullio, R. Poli and A. Debuigne, *Macromolecules*, 2013, 46, 4303–4312.
46 A. Debuigne, A. N. Morin, A. Kermagoret, Y. Piette, C. Detrembleur, C. Jerome and R. Poli, *Chem. – Eur. J.*, 2012, 18, 12834–12844.
47 M. Dréan, A. Debuigne, C. Jérôme, C. Goncalves, P. Midoux, J. Rieger and P. Guégan, *Macromol. Biosci.*, 2018, 18, 1700353.
48 M. Fineman and S. D. Ross, *J. Polym. Sci.*, 1950, 5, 259–262.
49 T. Kelen and F. Tudos, *J. Macromol. Sci., Part A: Pure Appl. Chem.*, 1975, 9, 1–27.
50 A. Wamsley, B. Jasti, P. Phiasivongsa and X. Li, *J. Polym. Sci., Part A: Polym. Chem.*, 2004, 42, 317–325.
51 J. M. Ting, T. S. Navale, F. S. Bates and T. M. Reineke, *ACS Macro Lett.*, 2013, 2, 770–774.
52 I. Skeist, *J. Am. Chem. Soc.*, 1946, 68, 1781–1784.
53 A. Debuigne, J. R. Caille and R. Jérôme, *Macromolecules*, 2005, 38, 5452–5458.

Published in : Polymer Chemistry (2019), vol. 10, n°23, pp. 3055–3065
DOI: 10.1039/c9py00020h
Status : Postprint (Author's version)

54 S. Maria, H. Kaneyoshi, K. Matyjaszewski and R. Poli, *Chem. – Eur. J.*, 2007, 13, 2480–2492.

55 A. Debuigne, R. Poli, R. Jerome, C. Jerome and C. Detrembleur, *ACS Symp. Ser.*, 2009, 1024, 131–147.

56 R. Bryaskova, N. Willet, A. Debuigne, R. Jérôme and C. Detrembleur, *J. Polym. Sci., Part A: Polym. Chem.*, 2007, 45, 81–89.

57 O. L. Wheeler, S. L. Ernst and R. N. Crozier, *J. Polym. Sci.*, 1952, 8, 409–423.

58 R. D. Lousenberg and M. S. Shoichet, *Macromolecules*, 2000, 33, 1682–1685.